

Quarkonium spectra with magnetically-induced anisotropic confinement

Ahmad Jafar Arifi^{1,2,*} and Kei Suzuki^{1,†}

¹*Advanced Science Research Center, Japan Atomic Energy Agency, Tokai 319-1195, Japan*

²*Research Center for Nuclear Physics, The University of Osaka, Ibaraki, Osaka 567-0047, Japan*

(Dated: March 16, 2026)

Strong magnetic fields modify the force that confines quarks inside hadrons and make it direction-dependent. Using quark-antiquark potentials obtained from lattice simulations as inputs to a quark potential model, we investigate how the anisotropic confinement affects the mass spectrum of quarkonium. In the strong-field regime, we find downward mass shifts induced by a softening of the confining potential along the field direction. In particular, the mass shifts of radially excited states are more significant than that of the ground state. For the longitudinal spin eigenstates, the excited-state spectrum strongly depends on the magnetic-field strength, in contrast to the spectrum with conventional isotropic confinement, which is insensitive to the field strength. This provides a clean probe of magnetically induced confinement anisotropy that can be confirmed in future lattice simulations.

Introduction. Understanding how fundamental interactions respond to external influences is a recurring theme across many areas of physics. In strongly interacting systems, such external influences are particularly informative, as they offer new opportunities to explore the formation of bound states and the response of their internal dynamics to changes in the surrounding environment [1–3]. Quantum chromodynamics (QCD), the theory of the strong interaction, remains not fully understood under external conditions, making it a compelling subject for investigation. Because QCD is inherently nonperturbative at hadronic scales, first-principles numerical approaches, i.e., lattice QCD simulations, play a central role in revealing the mechanisms of confinement [4–6] and hadron properties [7–22] in magnetic fields.

Lattice QCD simulations have shown that a strong magnetic field induces a pronounced anisotropy in the quark-antiquark potential [4, 5], which has recently been explored up to $eB = 9 \text{ GeV}^2$ [6]. In particular, the confining force becomes stronger transverse to the magnetic field and weaker along it, as illustrated schematically in Fig. 1(a), while the accompanying anisotropy of the short-range Coulomb interaction was found to be small [5]. This naturally raises the question of how hadronic bound states respond when the underlying interaction becomes anisotropic.

Heavy quarkonia provide a particularly clean framework for addressing this problem. As nonrelativistic bound states characterized by well-separated energy scales, their spectra are tightly governed by the shape of the interquark potential [23–25]. Radially excited states, which probe larger spatial regions, are therefore especially sensitive to anisotropic deformations of the confining interaction, making them powerful probes of directional modifications induced by strong magnetic fields.

The properties of quarkonia in external magnetic fields, both static [26–62] and dynamical [63–69], have been extensively investigated. However, the specific impact of magnetically induced anisotropy of the confining potential itself has received comparatively less attention [35, 70–77].

Motivated by recent lattice QCD results on anisotropic confinement [4–6], in this work we explore how such anisotropy manifests itself in the quarkonium spectrum. By employing anisotropic string tensions as inputs to a quark potential model [37, 38], we find substantial and robust modifications of the level spacing, with particularly large downward shifts of radially excited states driven primarily by the weakened longitudinal confinement. While earlier quark-model study [35] focused mainly on the weak-field regime and radial ground states, where anisotropic Coulomb effects play a more prominent role. More recent lattice QCD result [6] enables a systematic investigation of spectral modifications in the strong-field regime. In this region, excited quarkonium states provide especially sensitive probes of anisotropic confinement and offer clear insight into the directional restructuring of the strong interaction under extreme conditions.

Model. We first present the calculation of quarkonium spectra within a simple quark model under a static and uniform magnetic field $\mathbf{B} = B\hat{z}$, taking charmonium as a representative example. The Hamiltonian for the two-body system consisting of charm and anticharm quarks is

$$H_{c\bar{c}} = \sum_{i=c,\bar{c}} \left[m_i + \frac{(\mathbf{p}_i - q_i \mathbf{A})^2}{2m_i} - \boldsymbol{\mu}_i \cdot \mathbf{B} \right] + V_{c\bar{c}}(r), \quad (1)$$

where m_i , \mathbf{p}_i , and q_i are the quark mass, momentum, and electric charge, respectively. We adopt the symmetric gauge $\mathbf{A} = \frac{1}{2} \mathbf{B} \times \mathbf{r}$ and use the quark magnetic moment $\boldsymbol{\mu}_i = gq_i \mathbf{S}_i / (2m_i)$ with the Landé g-factor $g = 2$.

The quark-antiquark interaction is modeled as

$$V_{c\bar{c}}(r) = C + \sigma r - \frac{\alpha}{r} + \beta(\mathbf{S}_c \cdot \mathbf{S}_{\bar{c}})e^{-\Lambda r^2}, \quad (2)$$

* aj.arif01@gmail.com

† k.suzuki.2010@th.phys.titech.ac.jp

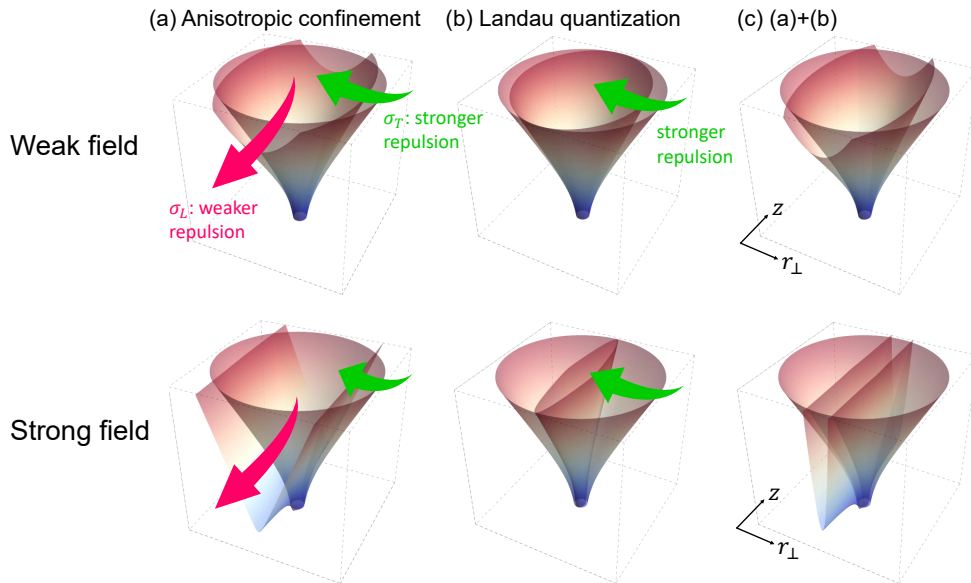


FIG. 1. Schematics of magnetic-field-induced anisotropy effects in quarkonia in the weak- and strong-field regimes: (a) anisotropic confinement potential, (b) harmonic-oscillator potential arising from Landau quantization of quarks, and (c) the sum of both contributions. The conventional isotropic (i.e., linear and Coulomb) potential is also plotted for comparison.

where $r = \sqrt{z^2 + r_\perp^2}$ is the relative distance. The parameters σ , α , and β represent the confining, Coulomb, and spin-spin interactions, and Λ controls Gaussian smearing of the spin-spin potential [78]. The constant C fixes the overall mass shift. For the model parameters, we use the same set as Refs. [37, 38]: $m_c = 1.784$ GeV, $\alpha = 0.713$ GeV, $\sqrt{\sigma} = 0.402$ GeV, $\beta = 0.4778$ GeV, $\Lambda = 1.020$ GeV², $C = -0.5693$ GeV, and $q_c = -q_{\bar{c}} = (2/3)e$ with the elementary charge e .

For charmonia (i.e., two-particle systems of equal masses and opposite electric charges) with vanishing pseudo-momentum, the Hamiltonian reduces to a relative form [30, 31, 79]:

$$H = -\frac{\nabla^2}{2\mu} + \frac{q^2 B^2}{8\mu} r_\perp^2 + V(r) - \sum_{i=c,\bar{c}} \boldsymbol{\mu}_i \cdot \mathbf{B}, \quad (3)$$

where $\mu = m_c/2$ and $q = (2/3)e$. The $B^2 r_\perp^2$ term represents the quark-Landau-level contribution and preserves cylindrical symmetry, as illustrated in Fig. 1(b).

The last term in Eq. (3), the quark Zeeman effect, leads to mixing between the pseudoscalar quarkonia $|00\rangle$ and the longitudinal spin component $|10\rangle$ of vector quarkonia, where the state is labeled by $|SS_z\rangle$ with the total spin S and its third component S_z , while the transverse components $|S_z = \pm 1\rangle$ remain decoupled. The off-diagonal matrix element is

$$\langle 10 | -(\boldsymbol{\mu}_1 + \boldsymbol{\mu}_2) \cdot \mathbf{B} | 00 \rangle = -\frac{gqB}{4\mu}, \quad (4)$$

which produces a coupled-channel Schrödinger equation for the $S_z = 0$ sector. Due to this mixing, the longitudinal states are labeled as the 1st, 2nd, 3rd, 4th, etc.,

while the transverse states are labeled $J/\psi_T, \psi'_T$, and so forth. Then, we solve the Schrödinger equation using the *cylindrical Gaussian expansion method* (CGEM) [37, 38], an extension of the Gaussian expansion method [80, 81] optimized for systems with cylindrical symmetry, which allows accurate determination of spectra and wave functions in magnetic fields.

Anisotropy. Lattice QCD simulations show that strong magnetic fields deform the string tension, where the transverse confinement is enhanced while the longitudinal one is suppressed [4–6]. We first model the

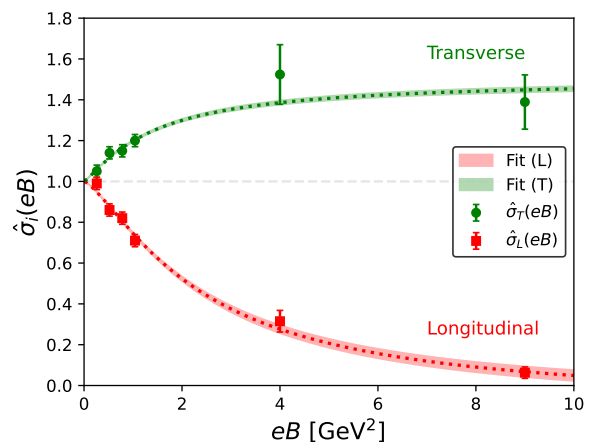


FIG. 2. Magnetic-field-induced anisotropy of the string tension, extracted from our fits and compared with available lattice-QCD results [5, 6], where we put the four data points at the finest lattice spacing $a = 0.0989$ fm in Ref. [5] and the two data at $eB = 4, 9$ GeV² in Ref. [6].

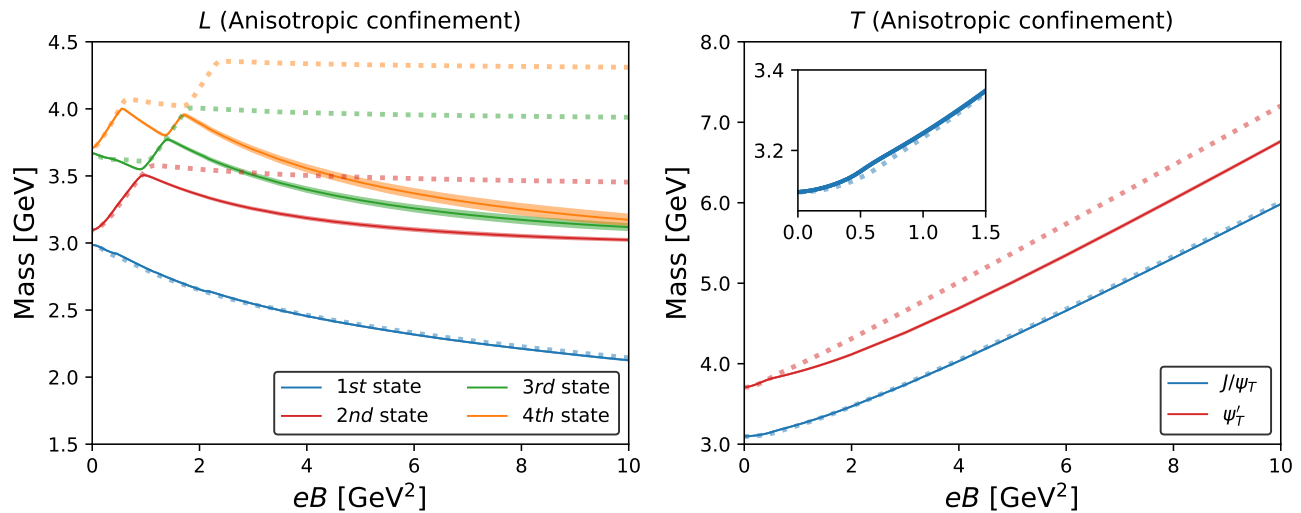


FIG. 3. Charmonium mass spectrum as a function of the magnetic-field strength eB under anisotropic confinement. The left and right panels correspond to longitudinal ($S_z = 0$) and transverse ($S_z = \pm 1$) charmonia, respectively. Dotted lines are the numerical results with the isotropic potentials.

anisotropic linear confinement as

$$V_{\text{conf}}^{\text{aniso}}(r_{\perp}, z) = \sigma(0) \sqrt{\epsilon_L z^2 + \epsilon_T r_{\perp}^2}, \quad (5)$$

where $\epsilon_{T,L}$ are related to the transverse and longitudinal string tensions via $\sigma_{T,L}/\sigma(0) = \sqrt{\epsilon_{T,L}}$. The magnetic-field dependence of the normalized string tensions $\hat{\sigma}_i(eB) = \sigma_i(eB)/\sigma(0)$ is parametrized as

$$\hat{\sigma}_i(eB) = 1 + \frac{\zeta_i(eB)^{\gamma_i}}{1 + \kappa_i(eB)^{\gamma_i}}, \quad i = T, L, \quad (6)$$

which exhibits saturation behavior at large eB . Here, ζ_i and κ_i determine the overall magnitude of the anisotropy, while γ_i regulates the steepness of its dependence on the magnetic field. Here, we obtain the model parameters

$$(\zeta_T, \kappa_T, \gamma_T) = (0.329, 0.659, 1.186), \quad (7)$$

$$(\zeta_L, \kappa_L, \gamma_L) = (-0.333, 0.305, 1.344), \quad (8)$$

that reproduce the overall trends of the lattice-QCD data as shown in Fig. 2. Here we assign a 2% error so as to obtain uncertainties comparable to lattice results for the longitudinal component at 9 GeV^2 . Although uncertainties of the lattice data for the transverse component are much larger, we also apply a 2% error, because we later find that its effect is insignificant and is effectively screened by Landau quantization.

Spectroscopy. Figure 3 demonstrates that the longitudinal ($S_z = 0$) and transverse ($S_z = \pm 1$) eigenstates of charmonia respond in qualitatively different ways to anisotropic confinement in strong magnetic fields, revealing a striking pattern compared with the isotropic case. We find that pronounced downward mass shifts develop for excited charmonia, while the ground state is relatively insensitive. As a result, the avoided crossings between

excited states are shifted to smaller values of both eB and the masses, which has important implications for determining the nonadiabatic transition rates in transient magnetic fields [69].

The downward mass shifts for the ground and excited states originate from the reduction of the longitudinal string tension [6], which weakens confinement along the magnetic-field direction and extends the wave function longitudinally, thereby lowering the excitation energies. At the same time, transverse squeezing plays a minor role, because its effect is almost screened by the freezing of transverse motion into the lowest Landau level (LLL), as illustrated in Fig. 1(c). However, in the weak-field regime, where the Landau quantization is less significant, the mass increases due to the enhancement of transverse confinement, although this effect is rather small, as shown in the inset of the right panel in Fig. 3.

This behavior contrasts with the isotropic potential case [37, 38], shown by the dotted lines in Fig. 3. In that scenario, the masses of excited longitudinal charmonia saturate at large eB once the transverse motion is frozen into the LLL and spin mixing [Eq. (4)] reaches its asymptotic limit. Then, due to the cancellation between the positive eB dependence of the LLL energy and the negative Zeeman shift, the spectrum in the strong- eB regime is flattened into a constant plateau, whereas the masses of transverse charmonia continue to increase due to the LLL energy in the absence of Zeeman shifts. Note that such a flattening mechanism is also expected to hold for the ground state; however, it has not yet saturated for charmonium in the current plot range, while this saturation can be seen in the light-meson sector [82–85].

Although our calculation is based on a nonrelativistic framework, the same saturation mechanism holds even in the relativistic picture. The relativistic Landau levels

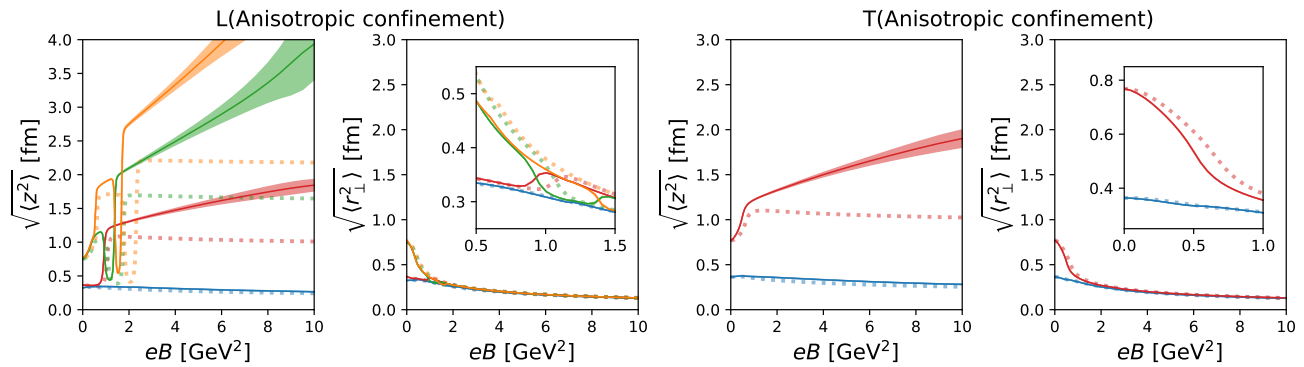


FIG. 4. Root-mean-square longitudinal and transverse radii, $\sqrt{\langle z^2 \rangle}$ and $\sqrt{\langle r_{\perp}^2 \rangle}$, as functions of the magnetic field eB , for anisotropic confinement. Dotted lines are the numerical results with the isotropic potentials.

for Dirac fermions are represented as [86, 87]

$$E_{n,s} = \sqrt{p_z^2 + m^2} + |qB|(2n + 1 - s). \quad (9)$$

This form contains the Zeeman shift through the spin index s and implies that the relativistic LLL ($n = 0$, $s = +1$) is independent of the magnetic field. Since quarkonia in the $B \rightarrow \infty$ limit are dominated by the LLLs of the quark and antiquark, the saturated energy can be written as

$$E_{||}(B \rightarrow \infty) \approx \sqrt{p_{z,1}^2 + m^2} + \sqrt{p_{z,2}^2 + m^2}. \quad (10)$$

For discussion on neutral light mesons, also see Refs. [82–85].

The anisotropic case is therefore qualitatively distinct: because the longitudinal potential itself is modified, the spectrum continues to evolve even in regimes where isotropic systems have already saturated. We conclude that the magnetic-field dependence of excited-state masses provides a clear and robust signal of the weakened longitudinal confinement.

Deformation. Figure 4 illustrates the magnetic-field dependence of charmonium radii, defined as $\sqrt{\langle z^2 \rangle} \equiv \sqrt{3\langle \psi | z^2 | \psi \rangle}$ and $\sqrt{\langle r_{\perp}^2 \rangle} \equiv \sqrt{(3/2)\langle \psi | r_{\perp}^2 | \psi \rangle}$ [37, 38]. In the isotropic case (dotted lines), the transverse radius is strongly suppressed by Landau-level squeezing, while the longitudinal radius remains nearly unchanged at large eB . This behavior reflects that the transverse motions of quarks are frozen into the LLL, while the longitudinal motion is not affected.

When anisotropic confinement [Eq. (5)] is introduced, the radii of the excited states undergo substantial modifications, as shown in Fig. 4. The magnetic field significantly weakens the longitudinal confinement, producing a much shallower potential along the field direction. As a result, the quarkonium wave function becomes strongly elongated longitudinally, leading to a large increase in $\sqrt{\langle z^2 \rangle}$. This elongation is more pronounced for higher radial excitations, since their larger size is more sensi-

tive to the weakened confinement. The large uncertainty further reflects the strong sensitivity to the anisotropy.

In strong magnetic fields, although the transverse confinement is enhanced, its effect remains subdominant compared with the Landau-level squeezing, and the transverse radius $\sqrt{\langle r_{\perp}^2 \rangle}$ is therefore nearly unaffected by the anisotropic confinement. In smaller magnetic fields, the strengthened transverse confinement becomes more visible, leading to a slight reduction of the transverse radius, as shown in Fig. 4.

Conclusion. In summary, we have explored how the lattice-QCD-motivated anisotropic confinement potential induced by strong magnetic fields [4–6] modifies the mass spectra and structure of charmonia by precisely solving a quark potential model. We find that the dominant effect originates from the substantial weakening of the longitudinal string tension, which leads to pronounced downward mass shifts of radially excited longitudinal charmonia, in sharp contrast to the characteristic mass plateau observed in the isotropic case in the strong magnetic-field regime. By comparison, the ground state is only mildly affected, which emphasizes the sensitivity of excited states to the anisotropic confinement. This reduced longitudinal confinement also induces a strong elongation of the wave function along the magnetic-field direction, as characterized by a significant increase in the longitudinal radius $\sqrt{\langle z^2 \rangle}$, whereas in the isotropic case the radius saturates. Thus, our results establish a transparent and quantitative connection between lattice-QCD results and quarkonium structure in extreme magnetic environments.

Acknowledgments. A. J. A. was supported by the JAEA Postdoctoral Fellowship Program, and partially by the RCNP Collaboration Research Network Program under Project No. COREnet 057, as well as by the PUTI Q1 Grant from the University of Indonesia under Contract No. PKS-206/UN2.RST/HKP.05.00/2025. This work was supported by the Japan Society for the Promotion of Science (JSPS) KAKENHI (Grant No. JP24K07034).

- [1] K. Hattori and X.-G. Huang, Novel quantum phenomena induced by strong magnetic fields in heavy-ion collisions, *Nucl. Sci. Tech.* **28**, 26 (2017), arXiv:1609.00747 [nucl-th].
- [2] J. Zhao, K. Zhou, S. Chen, and P. Zhuang, Heavy flavors under extreme conditions in high energy nuclear collisions, *Prog. Part. Nucl. Phys.* **114**, 103801 (2020), arXiv:2005.08277 [nucl-th].
- [3] S. Iwasaki, M. Oka, and K. Suzuki, A review of quarkonia under strong magnetic fields, *Eur. Phys. J. A* **57**, 222 (2021), arXiv:2104.13990 [hep-ph].
- [4] C. Bonati, M. D'Elia, M. Mariti, M. Mesiti, F. Negro, and F. Sanfilippo, Anisotropy of the quark-antiquark potential in a magnetic field, *Phys. Rev. D* **89**, 114502 (2014), arXiv:1403.6094 [hep-lat].
- [5] C. Bonati, M. D'Elia, M. Mariti, M. Mesiti, F. Negro, A. Rucci, and F. Sanfilippo, Magnetic field effects on the static quark potential at zero and finite temperature, *Phys. Rev. D* **94**, 094007 (2016), arXiv:1607.08160 [hep-lat].
- [6] M. D'Elia, L. Maio, F. Sanfilippo, and A. Stanzione, Confining and chiral properties of QCD in extremely strong magnetic fields, *Phys. Rev. D* **104**, 114512 (2021), arXiv:2109.07456 [hep-lat].
- [7] G. S. Bali, F. Bruckmann, G. Endrődi, Z. Fodor, S. D. Katz, S. Krieg, A. Schafer, and K. K. Szabo, The QCD phase diagram for external magnetic fields, *JHEP* **02**, 044, arXiv:1111.4956 [hep-lat].
- [8] E. V. Luschevskaya and O. V. Larina, The ρ and A mesons in a strong abelian magnetic field in $SU(2)$ lattice gauge theory, *Nucl. Phys. B* **884**, 1 (2014), arXiv:1203.5699 [hep-lat].
- [9] Y. Hidaka and A. Yamamoto, Charged vector mesons in a strong magnetic field, *Phys. Rev. D* **87**, 094502 (2013), arXiv:1209.0007 [hep-ph].
- [10] E. V. Luschevskaya, O. E. Solovjeva, O. A. Kochetkov, and O. V. Teryaev, Magnetic polarizabilities of light mesons in $SU(3)$ lattice gauge theory, *Nucl. Phys. B* **898**, 627 (2015), arXiv:1411.4284 [hep-lat].
- [11] E. V. Luschevskaya, O. E. Solovjeva, and O. V. Teryaev, Magnetic polarizability of pion, *Phys. Lett. B* **761**, 393 (2016), arXiv:1511.09316 [hep-lat].
- [12] G. S. Bali, B. B. Brandt, G. Endrődi, and B. Gläbke, Meson masses in electromagnetic fields with Wilson fermions, *Phys. Rev. D* **97**, 034505 (2018), arXiv:1707.05600 [hep-lat].
- [13] G. S. Bali, B. B. Brandt, G. Endrődi, and B. Gläbke, Weak decay of magnetized pions, *Phys. Rev. Lett.* **121**, 072001 (2018), arXiv:1805.10971 [hep-lat].
- [14] E. V. Luschevskaya, O. V. Teryaev, D. Y. Golubkov, O. V. Solovjeva, and R. A. Ishkuvatov, Tensor polarizability of the vector mesons from $SU(3)$ lattice gauge theory, *JHEP* **11**, 186, arXiv:1811.02344 [hep-lat].
- [15] K. Hattori and A. Yamamoto, Meson deformation by magnetic fields in lattice QCD, *PTEP* **2019**, 043B04 (2019), arXiv:1901.10182 [hep-lat].
- [16] R. Bignell, W. Kamleh, and D. Leinweber, Pion in a uniform background magnetic field with clover fermions, *Phys. Rev. D* **100**, 114518 (2019), arXiv:1910.14244 [hep-lat].
- [17] R. Bignell, W. Kamleh, and D. Leinweber, Pion magnetic polarisability using the background field method, *Phys. Lett. B* **811**, 135853 (2020), arXiv:2005.10453 [hep-lat].
- [18] H.-T. Ding, S.-T. Li, A. Tomiya, X.-D. Wang, and Y. Zhang, Chiral properties of (2+1)-flavor QCD in strong magnetic fields at zero temperature, *Phys. Rev. D* **104**, 014505 (2021), arXiv:2008.00493 [hep-lat].
- [19] H.-T. Ding, S.-T. Li, J.-H. Liu, and X.-D. Wang, Chiral condensates and screening masses of neutral pseudoscalar mesons in thermomagnetic QCD medium, *Phys. Rev. D* **105**, 034514 (2022), arXiv:2201.02349 [hep-lat].
- [20] G. Endrődi, QCD with background electromagnetic fields on the lattice: A review, *Prog. Part. Nucl. Phys.* **141**, 104153 (2025), arXiv:2406.19780 [hep-lat].
- [21] H.-T. Ding, J.-B. Gu, S.-T. Li, and R. Thakkar, Chiral condensates and screening masses of neutral pseudoscalar mesons from lattice QCD at physical quark masses, *Phys. Rev. D* **111**, 074513 (2025), arXiv:2501.11262 [hep-lat].
- [22] H.-T. Ding and D. Zhang, Chiral Properties of (2+1)-Flavor QCD in Magnetic Fields at Zero Temperature, (2026), arXiv:2601.18354 [hep-lat].
- [23] E. Eichten, K. Gottfried, T. Kinoshita, K. D. Lane, and T.-M. Yan, Charmonium: Comparison with Experiment, *Phys. Rev. D* **21**, 203 (1980).
- [24] W. Buchmüller and S. H. H. Tye, Quarkonia and Quantum Chromodynamics, *Phys. Rev. D* **24**, 132 (1981).
- [25] S. Godfrey and N. Isgur, Mesons in a relativized quark model with chromodynamics, *Phys. Rev. D* **32**, 189 (1985).
- [26] K. Marasinghe and K. Tuchin, Quarkonium dissociation in quark-gluon plasma via ionization in magnetic field, *Phys. Rev. C* **84**, 044908 (2011), arXiv:1103.1329 [hep-ph].
- [27] K. Tuchin, J/ψ dissociation in parity-odd bubbles, *Phys. Lett. B* **705**, 482 (2011), arXiv:1105.5360 [nucl-th].
- [28] D.-L. Yang and B. Müller, J/ψ production by magnetic excitation of η_c , *J. Phys. G* **39**, 015007 (2012), arXiv:1108.2525 [hep-ph].
- [29] K. Tuchin, Particle production in strong electromagnetic fields in relativistic heavy-ion collisions, *Adv. High Energy Phys.* **2013**, 490495 (2013), arXiv:1301.0099 [hep-ph].
- [30] C. S. Machado, F. S. Navarra, E. G. de Oliveira, J. Noronha, and M. Strickland, Heavy quarkonium production in a strong magnetic field, *Phys. Rev. D* **88**, 034009 (2013), arXiv:1305.3308 [hep-ph].
- [31] J. Alford and M. Strickland, Charmonia and bottomonia in a magnetic field, *Phys. Rev. D* **88**, 105017 (2013), arXiv:1309.3003 [hep-ph].
- [32] S. Cho, K. Hattori, S. H. Lee, K. Morita, and S. Ozaki, QCD sum rules for magnetically induced mixing between η_c and J/ψ , *Phys. Rev. Lett.* **113**, 172301 (2014), arXiv:1406.4586 [hep-ph].
- [33] D. Dudal and T. G. Mertens, Melting of charmonium in a magnetic field from an effective AdS/QCD model, *Phys. Rev. D* **91**, 086002 (2015), arXiv:1410.3297 [hep-th].
- [34] S. Cho, K. Hattori, S. H. Lee, K. Morita, and S. Ozaki, Charmonium Spectroscopy in Strong Magnetic Fields by QCD Sum Rules: S-Wave Ground States, *Phys. Rev. D* **91**, 045025 (2015), arXiv:1411.7675 [hep-ph].
- [35] C. Bonati, M. D'Elia, and A. Rucci, Heavy quarkonia in strong magnetic fields, *Phys. Rev. D* **92**, 054014 (2015),

- arXiv:1506.07890 [hep-ph].
- [36] A. V. Sadofyev and Y. Yin, The charmonium dissociation in an “anomalous wind”, *JHEP* **01**, 052, arXiv:1510.06760 [hep-th].
- [37] K. Suzuki and T. Yoshida, Cigar-shaped quarkonia under strong magnetic field, *Phys. Rev. D* **93**, 051502 (2016), arXiv:1601.02178 [hep-ph].
- [38] T. Yoshida and K. Suzuki, Heavy meson spectroscopy under strong magnetic field, *Phys. Rev. D* **94**, 074043 (2016), arXiv:1607.04935 [hep-ph].
- [39] M. Hasan, B. Chatterjee, and B. K. Patra, Heavy quark potential in a static and strong homogeneous magnetic field, *Eur. Phys. J. C* **77**, 767 (2017), arXiv:1703.10508 [hep-ph].
- [40] B. Singh, L. Thakur, and H. Mishra, Heavy quark complex potential in a strongly magnetized hot QGP medium, *Phys. Rev. D* **97**, 096011 (2018), arXiv:1711.03071 [hep-ph].
- [41] N. R. F. Braga and L. F. Ferreira, Heavy meson dissociation in a plasma with magnetic fields, *Phys. Lett. B* **783**, 186 (2018), arXiv:1802.02084 [hep-ph].
- [42] S. Iwasaki, M. Oka, K. Suzuki, and T. Yoshida, Hadronic Paschen–Back effect, *Phys. Lett. B* **790**, 71 (2019), arXiv:1802.04971 [hep-ph].
- [43] A. Jahan C. S., N. Dhale, S. Reddy P., S. Kesarwani, and A. Mishra, Charmonium states in strong magnetic fields, *Phys. Rev. C* **98**, 065202 (2018), arXiv:1803.04322 [nucl-th].
- [44] S. Iwasaki and K. Suzuki, Quarkonium radiative decays from the hadronic Paschen–Back effect, *Phys. Rev. D* **98**, 054017 (2018), arXiv:1805.09787 [hep-ph].
- [45] M. Hasan, B. K. Patra, B. Chatterjee, and P. Bagchi, Landau Damping in a strong magnetic field: Dissociation of Quarkonia, *Nucl. Phys. A* **995**, 121688 (2020), arXiv:1802.06874 [hep-ph].
- [46] N. R. F. Braga and L. F. Ferreira, Quasinormal modes for quarkonium in a plasma with magnetic fields, *Phys. Lett. B* **795**, 462 (2019), arXiv:1905.11309 [hep-ph].
- [47] M. Hasan and B. K. Patra, Dissociation of heavy quarkonia in a weak magnetic field, *Phys. Rev. D* **102**, 036020 (2020), arXiv:2004.12857 [hep-ph].
- [48] J. Zhou, X. Chen, Y.-Q. Zhao, and J. Ping, Thermodynamics of heavy quarkonium in a magnetic field background, *Phys. Rev. D* **102**, 086020 (2020), arXiv:2006.09062 [hep-ph].
- [49] N. R. F. Braga and R. da Mata, Configuration entropy description of charmonium dissociation under the influence of magnetic fields, *Phys. Lett. B* **811**, 135918 (2020), arXiv:2008.10457 [hep-th].
- [50] N. R. F. Braga, Y. F. Ferreira, and L. F. Ferreira, Configuration entropy and stability of bottomonium radial excitations in a plasma with magnetic fields, *Phys. Rev. D* **105**, 114044 (2022), arXiv:2110.04560 [hep-th].
- [51] S. S. Jena, B. Shukla, D. Dudal, and S. Mahapatra, Entropic force and real-time dynamics of holographic quarkonium in a magnetic field, *Phys. Rev. D* **105**, 086011 (2022), arXiv:2202.01486 [hep-th].
- [52] J. Hu, S. Shi, Z. Xu, J. Zhao, and P. Zhuang, Magnetic field induced hair structure in the charmonium gluon dissociation, *Phys. Rev. D* **105**, 094013 (2022), arXiv:2202.07938 [nucl-th].
- [53] R. Ghosh, A. Bandyopadhyay, I. Nilima, and S. Ghosh, Anisotropic tomography of heavy quark dissociation by using the general propagator structure in a finite magnetic field, *Phys. Rev. D* **106**, 054010 (2022), arXiv:2204.02312 [hep-ph].
- [54] P. Parui, S. De, A. Kumar, and A. Mishra, QCD sum rule analysis of heavy quarkonium states in magnetized matter: Effects of magnetic and inverse magnetic catalysis, *Phys. Rev. D* **106**, 114033 (2022), arXiv:2208.05856 [hep-ph].
- [55] J. Sebastian, L. Thakur, H. Mishra, and N. Haque, Heavy quarkonia in QGP medium in an arbitrary magnetic field, *Phys. Rev. D* **108**, 094001 (2023), arXiv:2308.04410 [hep-ph].
- [56] I. Nilima, M. Hasan, B. K. Singh, and M. Y. Jamal, Quarkonia dissociation at finite magnetic field in the presence of momentum anisotropy, *Eur. Phys. J. C* **84**, 160 (2024), arXiv:2402.07848 [hep-ph].
- [57] S. S. Jena, J. Barman, B. Toniato, D. Dudal, and S. Mahapatra, A dynamical Einstein–Born–Infeld–dilaton model and holographic quarkonium melting in a magnetic field, *JHEP* **12**, 096, arXiv:2408.14813 [hep-th].
- [58] B. Shukla, J. Nongmaithem, D. Dudal, and S. Mahapatra, Interplay of magnetic field and chemical potential induced anisotropy and frame dependent chaos of a $Q\bar{Q}$ pair in holographic QCD, *Phys. Rev. D* **111**, 106002 (2025), arXiv:2411.17279 [hep-th].
- [59] L. Wen, M. Li, Y. Zhou, Y. Li, and J. P. Vary, Relativistic dynamics of charmonia in strong magnetic fields, *Phys. Rev. D* **112**, 014019 (2025), arXiv:2504.03294 [hep-ph].
- [60] S. S. Jena, A. Bhattacharjee, D. Dudal, and S. Mahapatra, Probing quarkonium diffusion in a magnetized quark–gluon plasma, *Phys. Rev. D* **112**, 086010 (2025), arXiv:2507.00746 [hep-th].
- [61] A. J. Arifi and K. Suzuki, Structure of heavy quarkonia in a strong magnetic field, *Phys. Rev. D* **112**, 094013 (2025), arXiv:2507.18894 [hep-ph].
- [62] C. A. Dominguez, M. Koning, and L. A. Hernández, Magnetic catalysis of charmonium in the vector channel, *Phys. Rev. D* **112**, 094049 (2025), arXiv:2510.09927 [hep-ph].
- [63] X. Guo, S. Shi, N. Xu, Z. Xu, and P. Zhuang, Magnetic field effect on charmonium production in high energy nuclear collisions, *Phys. Lett. B* **751**, 215 (2015), arXiv:1502.04407 [hep-ph].
- [64] K. Suzuki and S. H. Lee, Delayed versus accelerated quarkonium formation in a magnetic field, *Phys. Rev. C* **96**, 035203 (2017), arXiv:1610.09853 [hep-ph].
- [65] N. Dutta and S. Mazumder, Majorana flipping of quarkonium spin states in transient magnetic field, *Eur. Phys. J. C* **78**, 525 (2018), arXiv:1704.04094 [nucl-th].
- [66] J. Hoelck and G. Wolschin, Electromagnetic field effects on Υ -meson dissociation in PbPb collisions at LHC energies, *Eur. Phys. J. A* **53**, 241 (2017), arXiv:1712.06871 [hep-ph].
- [67] P. Bagchi, N. Dutta, B. Chatterjee, and S. P. Adhya, Dissociation of heavy quarkonium states in a rapidly varying strong magnetic field, *Mod. Phys. Lett. A* **38**, 2350035 (2023), arXiv:1805.04082 [nucl-th].
- [68] S. Iwasaki, D. Jido, M. Oka, and K. Suzuki, Survival probabilities of charmonia as a clue to measure transient magnetic fields, *Phys. Lett. B* **820**, 136498 (2021), arXiv:2104.13989 [hep-ph].
- [69] A. J. Arifi and K. Suzuki, Landau–Zener–Stückelberg–Majorana dynamics of magnetized quarkonia, (2025), arXiv:2512.24072 [hep-ph].
- [70] V. A. Miransky and I. A. Shovkovy, Magnetic catalysis

- and anisotropic confinement in QCD, *Phys. Rev. D* **66**, 045006 (2002), [arXiv:hep-ph/0205348 \[hep-ph\]](#).
- [71] M. N. Chernodub, QCD string breaking in strong magnetic field, *Mod. Phys. Lett. A* **29**, 1450162 (2014), [arXiv:1001.0570 \[hep-ph\]](#).
- [72] M. A. Andreichikov, V. D. Orlovsky, and Yu. A. Simonov, Asymptotic Freedom in Strong Magnetic Fields, *Phys. Rev. Lett.* **110**, 162002 (2013), [arXiv:1211.6568 \[hep-ph\]](#).
- [73] Y. A. Simonov and M. A. Trusov, Confinement and α_s in a strong magnetic field, *Phys. Lett. B* **747**, 48 (2015), [arXiv:1503.08531 \[hep-ph\]](#).
- [74] H. Bohra, D. Dudal, A. Hajilou, and S. Mahapatra, Anisotropic string tensions and inversely magnetic catalyzed deconfinement from a dynamical AdS/QCD model, *Phys. Lett. B* **801**, 135184 (2020), [arXiv:1907.01852 \[hep-th\]](#).
- [75] U. Gürsoy, M. Järvinen, G. Nijs, and J. F. Pedraza, On the interplay between magnetic field and anisotropy in holographic QCD, *JHEP* **03**, 180, [arXiv:2011.09474 \[hep-th\]](#).
- [76] I. Y. Aref'eva, K. Rannu, and P. Slepov, Energy Loss in Holographic Anisotropic Model for Heavy Quarks in External Magnetic Field, (2020), [arXiv:2012.05758 \[hep-th\]](#).
- [77] I. Y. Aref'eva, A. Hajilou, K. Rannu, and P. Slepov, Spatial Wilson Loops and Energy Loss for Heavy Quarks in Magnetized HQCD Model, (2026), [arXiv:2601.09611 \[hep-th\]](#).
- [78] T. Barnes, S. Godfrey, and E. S. Swanson, Higher charmonia, *Phys. Rev. D* **72**, 054026 (2005), [arXiv:hep-ph/0505002 \[hep-ph\]](#).
- [79] M. A. Andreichikov, B. O. Kerbikov, V. D. Orlovsky, and Y. A. Simonov, Meson spectrum in strong magnetic fields, *Phys. Rev. D* **87**, 094029 (2013), [arXiv:1304.2533 \[hep-ph\]](#).
- [80] M. Kamimura, Nonadiabatic coupled-rearrangement-channel approach to muonic molecules, *Phys. Rev. A* **38**, 621 (1988).
- [81] E. Hiyama, Y. Kino, and M. Kamimura, Gaussian expansion method for few-body systems, *Prog. Part. Nucl. Phys.* **51**, 223 (2003).
- [82] V. D. Orlovsky and Y. A. Simonov, Nambu-Goldstone mesons in strong magnetic field, *JHEP* **09**, 136, [arXiv:1306.2232 \[hep-ph\]](#).
- [83] H. Taya, Hadron Masses in Strong Magnetic Fields, *Phys. Rev. D* **92**, 014038 (2015), [arXiv:1412.6877 \[hep-ph\]](#).
- [84] M. A. Andreichikov, B. O. Kerbikov, E. V. Lushevskaya, Yu. A. Simonov, and O. E. Solovjeva, The Evolution of Meson Masses in a Strong Magnetic Field, *JHEP* **05**, 007, [arXiv:1610.06887 \[hep-ph\]](#).
- [85] T. Kojo, Neutral and charged mesons in magnetic fields: A resonance gas in a non-relativistic quark model, *Eur. Phys. J. A* **57**, 317 (2021), [arXiv:2104.00376 \[hep-ph\]](#).
- [86] I. I. Rabi, Das freie Elektron im homogenen Magnetfeld nach der Diracschen Theorie, *Z. Phys.* **49**, 507 (1928).
- [87] M. H. Johnson and B. A. Lippmann, Motion in a Constant Magnetic Field, *Phys. Rev.* **76**, 828 (1949).